Ninth International Conference on CFD in the Minerals and Process Industries
CSIRO, Melbourne, Australia
10-12 December 2012

LARGE EDDY SIMULATION OF A SOLID-LIQUID FLUIDIZED BED USING THE LATTICE-BOLTZMANN METHOD AND A SOFT-SPHERE COLLISION MODEL

J.-S. KROLL-RABOTIN*, R. SUNGKORN, S. A. HASHEMI, J. J. DERKSEN and R. S. SANDERS

Department of Chemical and Materials Engineering, University of Alberta, Edmonton AB, CANADA
*Corresponding author, E-mail address: jean-sebastien.kroll-rabotin@ualberta.ca

ABSTRACT

In this paper, a Lagrangian Particle Tracking (LPT) approach for the dynamic simulation of a solid-liquid fluidized bed is evaluated. This approach is based on Large Eddy Simulation (LES) of the liquid phase using Lattice-Boltzmann Method (LBM) along with Discrete Elements Method (DEM) to account for particle-particle and particle-wall interactions. Translational and rotational motions of particles are solved by taking into account forces due to drag, lift, added mass, pressure and stress gradients, gravitational acceleration, and hindrance effects due to the presence of other particles. The coupling between phases is done in the so-called four-way coupling manner. The limitation of using LBM to solve the locally averaged conservation equations is overcome by an extended LBM scheme. The implementation of this model allows the numerical scheme to handle a wide range of particle sizes, particle types and particle loadings from dilute to dense mixtures. Owing to its inherently high parallel efficiency, the present model opens possibilities for a more realistic simulation of such systems which will be difficult, if not impossible, for other models.

NOMENCLATURE

r_p : particle radius
ρ_p : particle density
D : pipe diameter
ρ_f : liquid density
ν : liquid viscosity
g : gravity
σ : contact force spring stiffness
k : coefficient of restitution of contact energy
f_C : Coulombic friction coefficient
Δt : time step
φ : volume fraction of solids
$\vec{u}$: liquid velocity
$\vec{v}_p, \vec{\omega}_p$: velocity and angular velocity of particles
$\mathrm{Re}_p = 2\frac{\|\vec{v}_p - \vec{u}\| r_p}{\nu}$: particulate Reynolds number
C_D, C_L, C_M : drag, lift and added mass coefficients
$\vec{F}_p, \vec{T}_p$: force and torque acting on a particle
$\vec{\mathbf{F}}_p$: backward coupling force from particles
f^{φ} : non-conservation term

INTRODUCTION

Liquid fluidization is commonly used in many industrial processes and applications such as fluidized bed reactors and bioreactors, particle classification and separation, fluidized bed heat exchangers (FBHX), leaching and water treatment (Yang, 2003; Gevrin et al., 2008).

The most important advantage of fluidized beds is the high level of mixing resulting in highly effective mass and heat transfers, which are favorable in many industrial processes. Besides their significant industrial applications, liquid fluidized beds are an important research topic in studying particle-particle and fluid-particle interactions (Gevrin et al., 2008).

Theoretical models for different parameters, such as bed expansion in fluidized bed, that do not make use of empirical values and coefficients are limited to an amount of spherical particles of the order of 10^4 at very low Reynolds number (Yang, 2003).

In a solid-liquid fluidized bed, velocity and concentration of both phases undergo fluctuations whose frequency and magnitude are crucially important in determining parameters such as solid and liquid mass and heat transfers, granular pressure, particle attrition and breakage (Pozo et al., 1993, Zenit and Hunt, 2000).

The performance of the models that have been developed to predict these parameters are usually unsatisfactory. This is mainly due to poor understanding of the nature of the mechanisms that produce velocity and concentration fluctuations. An example of such poor understanding is illustrated in the study of Zenit et al. (1997) where they compared the experimental collisional pressure data against many different modeling approaches.

In this paper, three-dimensional and time-dependent simulations of a solid-liquid fluidized bed using Lagrangian Particle Tracking (LPT) and Lattice-Boltzmann Method (LBM) have been performed. The simulation results were compared against experimental test cases and other numerical results from the literature.

MODEL DESCRIPTION AND SIMULATION

The approach that was used to compute the transient behaviour of a liquid fluidized bed relies on several methods which were already thoroughly detailed in the literature. It is based on a lattice-Boltzmann numerical scheme for the fluid flow coupled with Lagrangian tracking of particles. The coupling between phases is realized in the so-called four-way coupling. It includes the effects of fluid on particle dynamics, the effects of particles on hydrodynamics, the effects of the velocity disturbance in the fluid on a particle generated by other particle, and the effects due to collision between particles.

Fluid flow computation

The continuous liquid phase is modelled using an extended lattice-Boltzmann (LB) numerical scheme. Different from conventional LB schemes, the extended LB scheme solves the locally averaged conservation equations allowing a realistic simulation of particulate flows ranged

from dilute to dense volume fraction. The effects of subgrid-scale (SGS) motions on the hydrodynamics are modeled using the Smagorinsky SGS model, i.e., Large Eddy Simulation (LES).

Lattice Boltzmann Method

Eggels and Somers (1995) LB scheme has been extended to solve the locally averaged conservation equations (see Sungkorn and Derksen, 2012). Instead of computing the physical quantities at the fluid nodes by solving the conservation equations directly, it accounts for velocity distribution functions from one fluid node to another. This is achieved by defining a lattice in which fluid nodes are bound to a finite number of neighbours and may exchange density of probability with them between time steps. This implies that exchanges of density of probability can only follow a finite number of directions, constrained by the lattice definition. In the three-dimensional Eggels and Somers scheme, velocity is discretized in 18 directions following a face-centered-hyper-cubic (FCHC) lattice.
The collision operator is a local function applied to each lattice node that calculates the exchanges of velocity distributions with the neighbours depending on current lattice quantities. The solution of the conservation equations is achieved by defining the collision operator properly.

Large Eddy Simulation

In the fluidized bed case, the mesh size is constrained by the size of particles as the Lagrangian tracking relies on the assumption that the particles are small compared to the phenomena of interest and can be represented using the distributed-particle concept (Sungkorn and Derksen, 2012). In contrast to the point-particle concept in which particles do not occupy space in liquid, displacement of particles in liquid is taken into account in the distributed-particle concept. The mesh size must be coarse enough to keep the point-particle concept valid and fine enough to correctly resolve the liquid hydrodynamics. The fluid lattice is thus too coarse to be able to solve the small turbulent scales. The dissipation of energy via the turbulence must then be modelled. This is done by adjusting the local apparent viscosity to account for eddy viscosity term, following the Smagorinsky SGS model:

$$\nu_t = (C_S \Delta)^2 \sqrt{S^2} \qquad (1)$$

where C_S is the Smagorinsky constant, Δ is the filter width (here, it is set equal to grid spacing) and $\sqrt{S^2}$ the resolved deformation rate. Here, C_s is set to 0.10. It has been pointed out by Hu and Celik (2008) that the so-called pseudo- (or particle-induced) turbulence possess a universal energy spectrum, with identifiable power-law decay (with different exponent from the classical -5/3). The power law decay implies that the contribution of the small scale pseudo-turbulence can be modelled using a dedicated subgrid-scale model. For now, there is no reliable and accurate SGS model readily available for multiphase flows, which is why a Smagorinsky model is used here (with the chosen Smagorinsky constant). Its capability is justified by favourable results as will be shown later. A detailed description of the implementation of the Smagorinsky SGS model in the framework of LBM can be found in, for example, Derksen and Van den Akker (1999), and Sungkorn et al. (2011).

Liquid hydrodynamics

The LB scheme due to Eggels and Somers (1995) focuses only on single-phase flows. For the liquid hydrodynamics in liquid fluidized beds in which particles occupy significant amount of space in the liquid, the hydrodynamics of the liquid phase must be solved using the locally average conservation equations which cannot be recovered using conventional LB schemes. Hence we have reformulated the conservation equations. This results in the conservation equations resemble their single-phase conservation counterparts with an additional factor due to the presence of particles (f^{φ}). The factor due to the presence of particles are explicitly computed at each time step. Since we typically use an extremely small time step (in the order of 10^{-4} s), it can be argued that the change of the volume fraction is relatively small. More details about the new scheme can be found in Sungkorn and Derksen (2012). In summary, the conservation equations being solved in this work are in the forms:

$$\frac{\partial \rho_f}{\partial t} + \vec{\nabla} \cdot (\rho_f \vec{u}) = f^{\varphi} \qquad (2)$$

$$\frac{\partial \rho_f \vec{u}}{\partial t} + \vec{\nabla} \cdot (\rho_f \vec{u}\,\vec{u}) = \vec{\nabla} \cdot \Pi - \frac{1}{(1-\varphi) V_f} \vec{\mathbf{F}}_p + f^{\varphi} \vec{u} \qquad (3)$$

where

$$f^{\varphi} = \frac{\rho_f}{1-\varphi} \left(\frac{\partial (1-\varphi)}{\partial t} + \vec{u} \cdot \vec{\nabla} (1-\varphi) \right) \qquad (4)$$

f^{φ} is accounted by modifying the collision operator.
In the absence of robust turbulence modulation model that applies in a fluidized bed, turbulence modulation (interactions with the small flow scales) by the particles is not included, however the particles still contribute to increasing or decreasing turbulence via the momentum coupling with the solid phase.

Solid phase computation

The translational and rotational motions of individual particles are tracked by solving Newton's equation of motion. The effects of fluid on particle dynamics, the effects of particles on hydrodynamics, the effects of particles of the velocity disturbance in the fluid on a particle by other particles, and the effects due to collisions between particles are accounted for in our simulations. This results in a so-called four-way coupling.

Particle dynamics

The effects of the fluid on particles are modelled using Lagrangian tracking with the distributed-particle concept. The translational and rotational motions of particles are solved based on Newton's second law of motion. The net force acting on the particle includes the net gravity force $\mathbf{F_G}$, forces due to the stress and pressure gradients $\mathbf{F_S}$, drag force $\mathbf{F_D}$, slip-rotation lift $\mathbf{F_{LR}}$ and slip-shear lift $\mathbf{F_{LS}}$ forces and, added mass force $\mathbf{F_A}$. The model also includes the hindrance effect due to the presence of other particles (exponent β in equations (6) and (7)). The quantities between the particle centroid on the Lagrangian frame of reference and the liquid on the Eulerian frame of reference are interpolated using a trilinear interpolation scheme. The forces acting on particles are shortly described hereafter, all the details about their expressions can be found in Sommerfeld (2000). The effect of small fluid scales on the particles is neglected, which means that the simulated particle trajectory is filtered. However, in our whole set of simulations, the Stokes number remains between 20 and 50, and according to Pozorksi and Apte (2009), for such high Stokes numbers, small scales do not contribute significantly to the particle motion. That is why no random walk or other finer model was used in the simulations. To

make sure this is also true in our filtered flow, the Stokes number based on the LES turbulent viscosity was calculated:

$$\mathrm{St}=\frac{1}{18}\frac{\rho_p}{\rho_f}\mathrm{Re}_{p,t}=\frac{1}{18}\frac{\rho_p}{\rho_f}\frac{2r_p u}{\nu_t} \tag{5}$$

where ν_t/ν varies between 2 and 13, so Stokes number is between 1.5 and 10. A value of 1.5 may imply a small contribution from the filtered scales, but this value is only reached locally and even in this case, collisions will contribute significantly more to particle motion and energy dissipation.

Three different expressions for the drag coefficient (C_D) are triggered depending on particulate Reynolds number. Those are Stokes drag for $\mathrm{Re}_p<0.5$, Schiller and Naumann (1933) for $0.5\leq\mathrm{Re}_p<1000$ and turbulent drag with constant drag coefficient for $\mathrm{Re}_p\geq1000$. Hindrance by the solids is accounted by rescaling the drag force for a dilute media by $(1-\varphi)^{-\beta}$, where φ is the local volume fraction of solids and β is (Di Felice, 2007):

$$\beta=3.7-0.65\exp\left(-\frac{1.5-\log_{10}\mathrm{Re}_p}{2}\right) \tag{6}$$

Two lift forces are considered, one due to the shear in the fluid flow ($C_L^{(S)}$), and the other due to the relative rotation between the particles and the fluid ($C_L^{(R)}$). The actual laws that are used change for different flow regimes based on the particulate Reynolds number (Sommerfeld, 2000). The net gravity force acting on each particle is described with contribution from the local-average density of mixture. The effects of the pressure and stress gradients in the fluid on each particle is reformulated for the computational efficiency. The added mass force is taken into account with a coefficient (C_M). The translational motion of particle is solved in the form:

$$\begin{aligned}(\rho_p+C_M\rho_f)\frac{D\vec{v}_p}{Dt}=&\\ \frac{3}{8r_p}\rho_f C_D(1-\varphi_p)^{-\beta}\|\vec{u}-\vec{v}_p\|(\vec{u}-\vec{v}_p)&\\ +\frac{3}{4}\rho_f C_L^{(S)}(\vec{u}-\vec{v}_p)\times(\vec{\nabla}\times\vec{u})&\\ +\frac{3}{4r_p}\rho_f C_L^{(R)}\frac{\vec{\nabla}\times\vec{u}-\vec{\omega}_p}{\|\vec{\nabla}\times\vec{u}-\vec{\omega}_p\|}\times\|\vec{u}-\vec{v}_p\|(\vec{u}-\vec{v}_p)&\\ +\rho_f(1+C_M)\frac{D\vec{u}}{Dt}+(\rho_p-\bar{\rho})\vec{g}+(V_p)^{-1}\vec{F}_p&\end{aligned} \tag{7}$$

In equation (7), $\vec{F}_p$ contains all the forces acting on particles that do not come from their interactions with the fluid flow. In the case of the fluidized bed, these are the collisions.

The rotational motion is tracked by solving the following equation:

$$\begin{aligned}\frac{2}{5}r_p^2\rho_p\frac{d\vec{\omega}_p}{dt}=&\\ \frac{3}{8\pi}r_p^2\rho_f C_R|\vec{\nabla}\times\vec{u}-\vec{\omega}_p|(\nabla\times\vec{u}-\vec{\omega}_p)+(V_p)^{-1}\vec{T}_p&\end{aligned} \tag{8}$$

The effects of particle on the continuous fluid phase are done by exerting forces $\vec{\mathbf{F}}_p$ (i.e., drag, lift, added mass, forces due to pressure and stress gradients) and displacing the fluid through f^{φ} .

Soft Sphere Collisions

Contact forces are modelled using the Soft Sphere Collision (SSC) model which defines a relation between the contact force acting on a particle and the overlap of its original shape with external objects. The particles are spherical and their radii do not evolve over time, so the overlap can be seen as a particle deformation. In the glass bead fluidized bed, particles hardly deform. However, it is necessary for simulation stability to allow particles to overlap a little (< 5% of their radius), as it numerically relaxes their contact interactions which have really short time scales in the physical bed.

Normal and tangential contact forces are considered. Both force components are modelled through a spring stiffness and a damping coefficient. Moreover, a Coulomb-type friction law is applied to the tangential direction. The derivation of these numerical parameters from the physical collision parameters is explained by Van Der Hoef et al. (2006). The same approach is followed here, and the simulation is finally characterized by three parameters: the normal spring stiffness, the friction coefficient and a restitution coefficient. The restitution coefficient, with which the value of the damping coefficient is calculated, accounts for the energy that is dissipated during collisions due to the deformation of the particles (it is the ratio of the energy after collision over the energy before collision).

Quantity	Physical value	Simulation
r_p	1 mm	0.258
ρ_p	2540 kg/m³	20.3
D	10.2 cm	26,2
ρ_f	1000 kg/m³	8
ν	10^{-6} m²/s	10^{-5}
g	9.81 m/s	5.69×10^{-5}
σ	-	0.0516
k	-	0.97
f_C	-	0.3
Δt	150 µs	1

Table 1: Scaling of the LBM simulations.

Simulation setup

The coupling is thus achieved through a force balance on the solid phase and through an extension of the lattice-Boltzmann scheme for the liquid phase. The effect of the turbulence is included in the expression of the apparent turbulent viscosity of the liquid using Smagorinski SGS model. The interactions between solids and with the walls are simulated following the soft-sphere collision model. In the end, all the physics that play a significant role in the liquid fluidized bed are modelled in the simulation.

The simulations were performed for 2 mm glass beads fluidized with water in a 10.16 cm (in diameter) circular pipe. The scaling is indicated in Table 1. As the geometry is constrained by the discretization of space directions, the circular section of the pipe is approximated with steps. The grid resolution is also constrained. As the assumption of point particles is only valid if the beads are sufficiently smaller than the lattice, so that interpolation of fluid properties at the position of the particle center has physical meaning: local flow around particles is modeled in the expressions of the forces in Lagrangian tracking but does not impact fluid nodes directly. In the end, the fluid mesh in the pipe section is relatively coarse.

Fluid boundary conditions

For the fluid, bounce-back boundary conditions are used at the pipe walls. At the top of the domain, a zero-gradient condition is imposed, while inlet velocity is imposed by an immersed boundary condition.

Due to the coupling with the solid phase, it is not easy to impose the fluid velocity using a "bounce-back + momentum" expression. In this case, it is circumvented by using a zero-gradient condition associated to a forcing on the fluid nodes that is proportional to the error on the fluid velocity.

The expression of the forcing is as follows (in its non-dimensional form, so $\Delta t=1$):

$$\vec{F}_{\text{in}}=2\rho_{\text{f}}\left(\vec{u}_{\text{in}}-\vec{u}\right) \qquad (9)$$

The coefficient of proportionality is set to $2\rho_{\text{f}}$ according to Eggel and Somers' (1995) scheme, so that the applied forcing corresponds exactly to the amount of momentum that must be added to each fluid node. The imposed fluid velocity is set to $\vec{u}_{\text{in}}=\frac{1}{8}\sum_{\text{n}}\delta\vec{u}_0$, where δ equals to 1 in the domain and 0 outside, and n is the summation index over the eight nodes in the inlet plane that share either a face or a corner with the node at which velocity is set. $\vec{u}_0$ is constant. The imposed profile is thus mostly flat, but it has lower velocity near the walls. This avoids potential instabilities or production of waves that could come from the slight compressibility of the LBM scheme.

Boundary conditions for particles

Walls are accounted in the collisions in the same way as the particles. The contact force applied to particles is calculated based on the overlap between the walls and the particles which makes the walls behave like infinite radius particles that do not move.

This same boundary condition is used at the inlet and at the outlet, so that particles cannot go out of the domain. The outlet boundary does not play any significant role in the simulation as particles are nor supposed to reach the outlet in fluidized bed conditions. As the inlet behaves like a wall for particles but allows the liquid to go through, it acts like an ideal screen.

The wall seen by the particles is cylindrical, so that particle bouncing directions are consistent with the actual particle-pipe interaction. That means that, considering that bounce-back boundary condition is located halfway between two fluid nodes, the boundary condition for the fluid and the boundary condition for particles are not exactly at the same place. The staircase section of the fluid and the circular one for particles are chosen so that they have the same area (hence the pipe radius that is not a n integer number in Table 1). The effect of this boundary has been checked by running simulations with the actual cylindrical wall and some simulations with staircase boundaries for both fluid and particles. No perceivable effect was observed on Richardson-Zaki law.

Particle properties

The solid particles are supposed to model a glass bead bed, however, the prevalent parameters that play a role on the fluidization regime (homogenous or bubbly) are the particle diameters and densities, and the concentration of the bed (Patankar and Joseph, 2001). That means that the interaction of particles via collisions do not need to be simulated exactly provided that the basic behaviour of collisions is respected. Physically, the spring stiffness (σ) is not a property of the material and is hard to measure. Numerically, if the stiffness is too high, the particles bounce faster than what the time scheme supports, so the simulation becomes unphysical and unstable. Nevertheless, as the resulting physics are not so much sensitive to this parameter, it is only set so that particles do not overlap too much (less than 1 % of their radius). It is the same for restitution coefficient (k). As it does not need to be precisely set, a relatively high value is used to satisfy the intuitive behaviour that glass bead collisions do not consume much energy, but it is not scaled to match material properties. The values used in the simulations are indicated in Table 1.

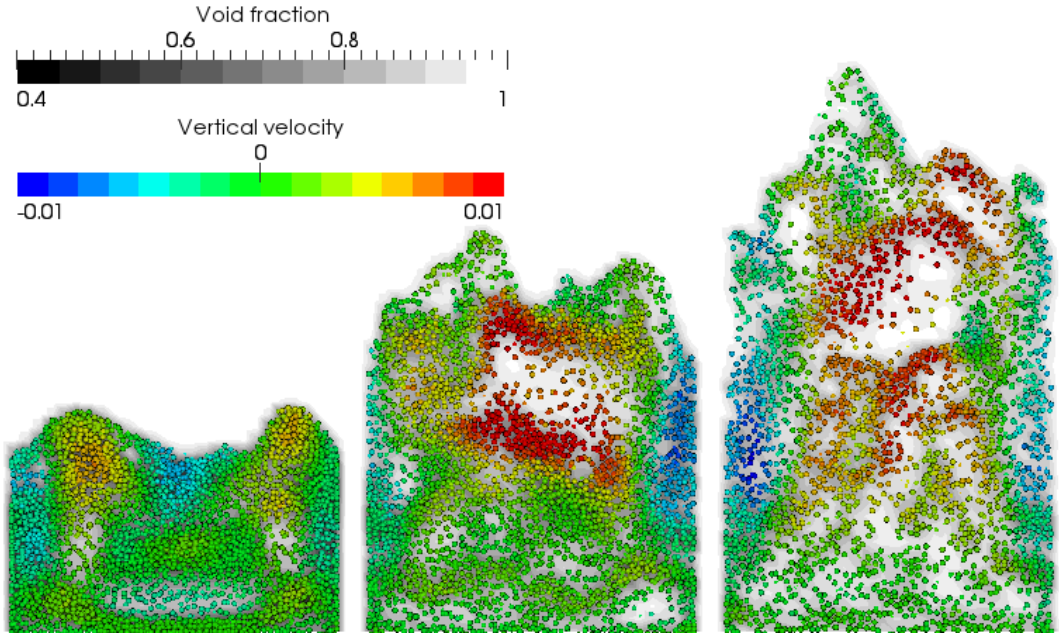

Figure 1: Snapshots of a central section of three fluidized beds with 45000 glass beads (cf. Table 1) at different fluidization velocities (9.45 cm/s, 15.25 cm/s and 18.14 cm/s) after steady state was reached

RESULTS

The simulation results were compared to experimental data of Hashemi (2012). He used a 10.16 cm (in diameter) fluidized bed to measure solids concentration and concentration fluctuations maps for 2 mm glass bead particles ($\rho_s = 2540$ kg/m³) at different fluidization velocities. Liquid superficial velocity was obtained using an orifice plate and differential pressure transducers. Solids instantaneous concentration distribution was measured using Industrial Tomography System (ITS) Z8000 high speed electrical impedance tomography (EIT) equipment along with a dual-plane tomography sensor. For each set of experiments, 8000 concentration maps were collected with the sampling rate of 820 Hz at each velocity from each sensor plane.

The experimental profiles showed lower concentration regions in the center of the bed. These lower concentration regions are also reported in the literature and correspond to bubbly structures in inhomogeneous liquid fluidized bed (Foscolo and Gibilaro, 1984; Patankar and Joseph, 2001). Foscolo and Gibilaro (1984) showed that at specific conditions, liquid fluidized bed will change from particulate to aggregate fluidized bed. In their experiments, this transition results in mushroom shape void fraction in the bed and produces low concentration regions at the center of the bed. According to their classification, the 2 mm glass bead liquid fluidized bed is in the transition region. This is illustrated by the numerical results presented in Figure 1 that show an inhomogeneous regime where bubbles do not have a well defined mushroom shape.

The Richardson-Zaki equation for hindered settling velocity has been widely used for solid-liquid fluidized beds (Yang, 2003):

$$u_{in} = u_t (1-\varphi)^n \qquad (10)$$

where u_{in}, u_t and φ are fluidization velocity, terminal settling velocity and solid average concentration. Based on Richardson-Zaki law, Zenit et al. (1997) determined the value of $n = 2.4$ for glass bead particles based on their experimental data. Figure 2 shows the comparison of fluidization velocity versus solids concentration for LBM simulations and Richardson-Zaki laws for 2 mm glass beads. The average concentration is calculated by averaging the time averaged concentration in a pipe section between the bottom and the top of the bed. Calculating the average velocity similarly, it matches the average imposed inlet velocity. The dashed line on the figure also shows a fitted Richardson-Zaki law with an exponent of 2.15. The results show a good agreement between experimental and numerical results with Richardson-Zaki law.

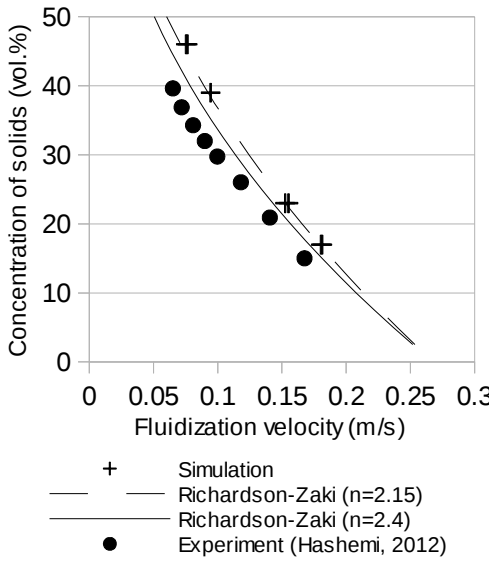

Figure 2: Comparision between simulation, experimental data and fitting with Richardson-Zaki

CONCLUSION AND PERSPECTIVES

A fully coupled simulation based on Discrete Element Method for the solids and Lattice-Boltzmann Method for the liquid has been used to simulate a liquid fluidized bed. It shows a relatively good agreement with the data available in the literature, both qualitatively and quantitatively.

The discrepancies can be explained by the coarse steps that describe the pipe wall boundary condition which is the major limitation of the simulation scheme. In future works, more modelling efforts will be necessary to model the pipe wall in a more physical way, such as using interpolated immersed boundary method (IBM). However, the preliminary results presented here are already really encouraging.

REFERENCES

DI FELICE, R., (2007), "Liquid suspensions of single and binary component solid particle: an overview",*China Particuology*, **5**, 312–320.

DERKSEN, J.J., and VAN DEN AKKER, H.E.A., (1999), "Large-eddy simulations on the flow driven by a Rushton turbine", *AIChE*, **39**, 1058-1069.

EGGELS, J.G.M., and SOMERS, J.A., (1995), "Numerical simulation of free convective flow using the lattice-Boltzmann scheme", *International Journal of Heat and Fluid Flow*, **16**, 357–364.

FOSCOLO, P. U. and GIBILARO, L. G., (1984), "A fully predictive criterion for the transition between particulate and aggregate fluidization", *Chemical Engineering Science*, **39** (12), 1667–1675.

GEVRIN, F., MASBERNAT, O. and SIMONIN, O., (2008), "Granular pressure and particle velocity fluctuations prediction in liquid fluidized beds", *Chemical Engineering Science*, **63** (9), 2450–2464.

HASHEMI, S. A., (2012), "Velocity and concentration fluctuations in concentrated solids-liquid flows", *PhD Thesis*, University of Alberta, Edmonton, AB, Canada.

HU, G. and CELIK, I., (2008), "Eulerian-Lagrangian based large-eddy simulation of a partially aerated flat bubble column", *Chemical Engineering Science*, **63**, 253-271 .

PATANKAR, N.A. AND JOSEPH, D.D., (2001), "Modeling and numerical simulation of particulate flows by the Eulerian-Lagrangian approach", *International Journal of Multiphase Flow*, **27**, 1659–1684 .

POZO, M.D., BRIENS, C.L. and WILD G., (1993), "Particle-particle collisions in liquid-solid and gas-liquid-solid fluidized beds", *Chemical Engineering Science*, **48** (18), 3313–3319.

POZORSKI, J. and APTE, S.V., (2009), "Filtered particle tracking in isotropic turbulence and stochastic modeling of subgrid-scale dispersion ", *International Journal of Multiphase Flow*, **35**, 118–128 .

SCHILLER, L. and NAUMANN, Z., (1933), "A drag

coefficient correlation", *VDI- Zeitschrift*, **77**, 318–320.

SOMMERFELD M., (2000), "Theoretical and experimental modeling of particulate flows", Lecture Series 2000–06. *von Karman Institute for Fluid Dynamics*, Belgium, April 3–7, 2000.

SUNGKORN R., DERKSEN J.J. and KHINAST J.G., (2011), "Modeling of turbulent gas–liquid bubbly flows using stochastic Lagrangian model and lattice-Boltzmann scheme ", *Chemical Engineering Science*, **66**, 2745–2757.

SUNGKORN, R. and DERKSEN, J.J., (2012), "Simulations of dilute sedimenting suspensions at finite-particle Reynolds numbers", *Physics of Fluids*, submitted.

VAN DER HOEF, M. A., YE, M. Ye, VAN SINT ANNALAND, ANDREWS, A.T., SUNDARESAN, S. and KUIPERS, J.A.M., (2006), "Multiscale Modeling Of Gas-Fluidized Beds ", *Advances in Chemical Engineering*, **31**, 65–149.

YANG W.C., (2003), editor, *Handbook of fluidization and fluid-particle systems*, 1st ed. Marcel Dekker, Inc.

ZENIT R., HUNT M.L., (2000), "Solid fraction fluctuations in solid-liquid flows", *International Journal of Multiphase Flow*, **26** (5), 763–781.

ZENIT R., HUNT M.L. and BRENNEN C.E., (1997), "Collisional particle pressure measurements in solid-liquid flows", *Journal of Fluid Mechanics*, **353**, 261–283.

